INTERFEROMETRIC GROUND NOTCHING

M. Mariotti d'Alessandro[1], S. Tebaldini[1], S. Quegan[2], M. Soja[3], L. M. H. Ulander[4]

[1] Politecnico di Milano, [2] University of Sheffield,
[3] University of Tasmania, [4] Chalmers University of Technology

ABSTRACT

The effectiveness of SAR tomography in estimating forest Above Ground Biomass (AGB) has been repeatedly demonstrated in the recent years. For tropical rain-forests, analysis from the Paracou test site reveals that the best results are achieved when the backscattered power coming from 30m above the ground is considered. As suggested in previous papers, the most likely reason is that ground scattering acts as a disturbing factor for forest biomass retrieval, as it depends on a number of parameters (like topography, moisture), that do not relate to forest biomass. In this paper we further test this hypothesis by proposing the concept of interferometric ground notching. By taking the difference between two phase calibrated, ground-steered, SAR SLC images a third image is obtained where ground scattering contributions are canceled out, hence the name ground-notched SLC. Results indicate that ground-notched data can effectively retain the features of vegetation-only scattering, including its polarimetric signature and correlation with AGB.

***Index Terms*—** InSAR, Polarimetry, Biomass, Tomography

1. INTRODUCTION

In the recent decades, understanding the Earth's dynamics has become a major topic among the scientific community. The development of accurate models demands increasingly accurate measurements of environmental variables. In particular, understanding climate change requires a quantitative characterization of the carbon cycle which in turn requires measurements of biomass. The use of remote sensing to estimate above ground biomass (AGB) has attracted much attention because of its potential for exploring large areas over relatively short times. A wide range of the electromagnetic spectrum has been used to infer biomass, but this paper focuses on estimation P-band SAR data. Existing estimation algorithms take advantage of polarization diversity [1] [2], interferometric pairs or tomographic stacks [3]. In particular, TomoSAR observables have shown excellent agreement with AGB, especially the backscattered power in the HV channel at 30m above ground level [4]. This can be ascribed to the removal of the ground echo, given its strong dependency on local topography and soil roughness and moisture rather than AGB alone. This paper describes the rejection of the ground echo by means of an interferometric technique using just two coherent radar images. Physical evidence and high correlation with AGB justify the proposed processing chain.

The growing interest in accurate global AGB maps motivated proposal for a dedicated satellite mission, and from several candidates, a P-band SAR radar, BIOMASS, was selected as the seventh ESA Earth Explorer. Orbit is planned to accomodate two separate phases based on tomography and interferometry. The tomographic phase will deliver an AGB map by jointly processing data from 7 repeat passes with 3-day spacing, whereas the interferometric phase will use only three images. Both will provide global AGB maps, the former in about 14 months and the latter in 7 months. The algorithm proposed in this paper aims to merge the fast revisit time of interferometric processing and the estimation accuracy of SAR tomography.

2. INTERFEROMETRIC GROUND NOTCH

Interferometric SAR processors rely on a pair of SAR images of the same target acquired from slightly different positions. The separation of the sensors is known as the baseline; the component of the baseline orthogonal to the line of sight is referred to as the normal baseline. The larger the normal baseline the stronger the sensitivity of the system in the vertical direction. Elevation information is embedded in the interferometric phase, which is the phase difference between the two images. The large distance of the sensors from the target means that the relationship between phase and elevation is approximately linear, k_z being the coefficient of proportionality. In other words, targets placed at the same distance from the reference (master) sensor are characterized by an interferometric phase dependent on their elevations. Any elevation, z, can be associated with an interferometric phase, φ, but the opposite does not hold due to the periodicity of the phase. The set of elevations associated with a fixed φ are given by $z + n \cdot z_{2\pi}$ with $n \in \mathbb{N}$; here $z_{2\pi}$ is the ambiguity height. Targets at elevations with zero interferometric phase can be emphasized by a coherent sum of the two images, while targets at half the ambiguity height are canceled.

Working with long waves and semi-transparent targets causes

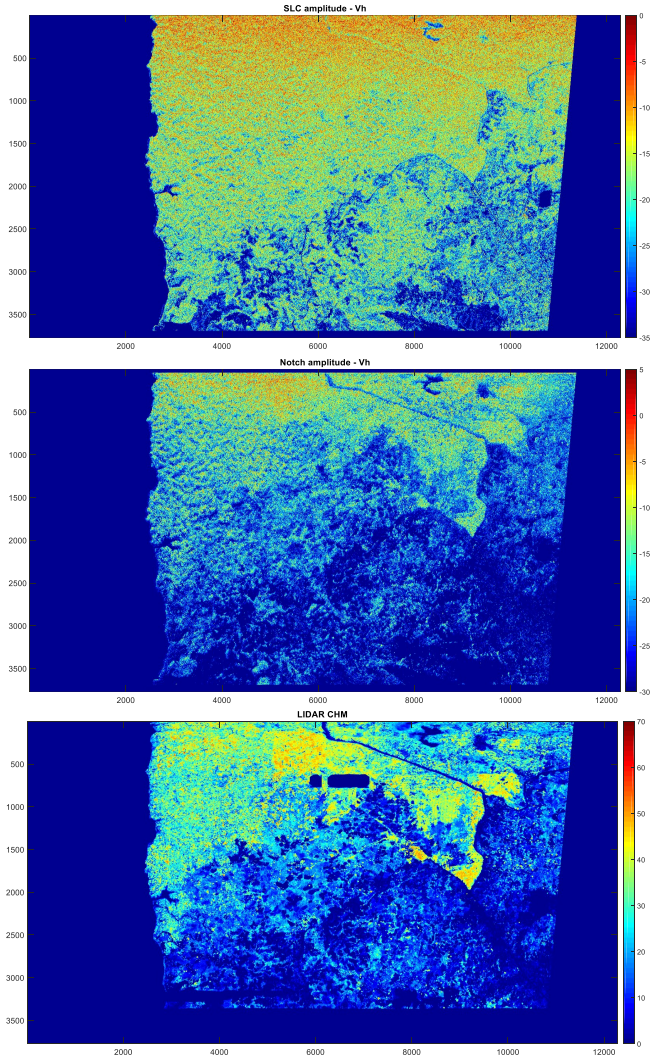

Fig. 1. From top to bottom: SLC power [dB], notch power [dB] and LIDAR derived Canopy Height Model (CHM) for the Mondah site.

many elevations to be imaged together so that they contribute to the same range-azimuth bin. After coregistration and ground steering, the complex value of the corresponding pixel in the master and slave image can be expressed as [5]:

$$y_M(r,a) = \int s(r,a,z)\,dz \quad (1)$$

$$y_S(r,a) = \int s(r,a,z)\cdot e^{j\cdot k_z\cdot z} dz \quad (2)$$

where $s(r,a,z)$ is a function describing the complex vertical reflectivity profile of the target. The difference between y_M and y_S produces the *ground notch* image y_{notch} whose power can be computed given knowledge of the statistical properties of $s(r,a,z)$. $s(r,a,z)$ can be modeled as a circularly symmetric normal distribution with zero mean and second order statistics given by equation (3).

$$\mathbb{E}\left[s(z)\,s^*(\zeta)\right] = \sigma_s^2(z)\,\delta(z-\zeta) \quad (3)$$

According to (3) and neglecting any decorrelation source, the expected power of the notch image is given by (4).

$$\mathbb{E}\left[|y_{notch}|^2\right] = 2\int \sigma_s^2(z)\cdot(1-cos(k_z\cdot z))\cdot dz \quad (4)$$

Equation (4) states that the power of the notch image is the integral of the vertical power of the target shaped by a $1-cos(k_z\cdot z)$ function. The vertical power profile is emphasized for elevations around $z_{2\pi}/2 + n\cdot z_{2\pi}$ and attenuated for those around $n\cdot z_{2\pi}$.

It must be remarked that in order to use this technique to remove the ground signal, the ground topography must be known. The consequence of imperfect ground steering is the presence of a signal coming from ground level in the notch image. In this work the technique detailed in [6] has been used: it jointly exploits tomography and polarimetry for separating ground and vegetation.

3. RESULTS

As a support activity for the BIOMASS mission many airborne campaigns on tropical forests have been carried out in recent years. Forests in South America and Africa have been imaged during TropiSAR [7] and AfriSAR [8] campaigns; results presented in this section come from these datasets. Each site is associated with a fully polarimetric tomographic stack acquired at P-band; the number of images varies from 6 to 10 providing vertical resolution going from approximately 5m to 20m . The vertical resolution fluctuates along azimuth because of platform deviations and degrades with range; as a consequence, notch results vary according to the particular image pair selected. However, overall platform stability is good, so associated values of k_z are stable and intra- and inter-image fluctuations are hardly noticeable.

In order to prove the effectiveness of the ground notch approach two main results are shown here. The first one is the appearance of features unconnected with the ground backscatter, while the second is the disappearance of scattering mechanisms that involve the ground. The middle panel of figure (1) shows the amplitude in the HV polarimetric channel of the notch image computed in accordance with the procedure outlined in section 2. The bottom panel of figure (1) shows forest top height estimated with LIDAR measurements [9]; high correlation between notch amplitude and forest height can be seen. As a comparison the amplitude associated with a single SLC image is shown at the top of figure (1), which illustrates that the correlation with forest height drops if a single image is used.

When imaging a forest with longer wavelengths a relevant fraction of the received power can be associated with the

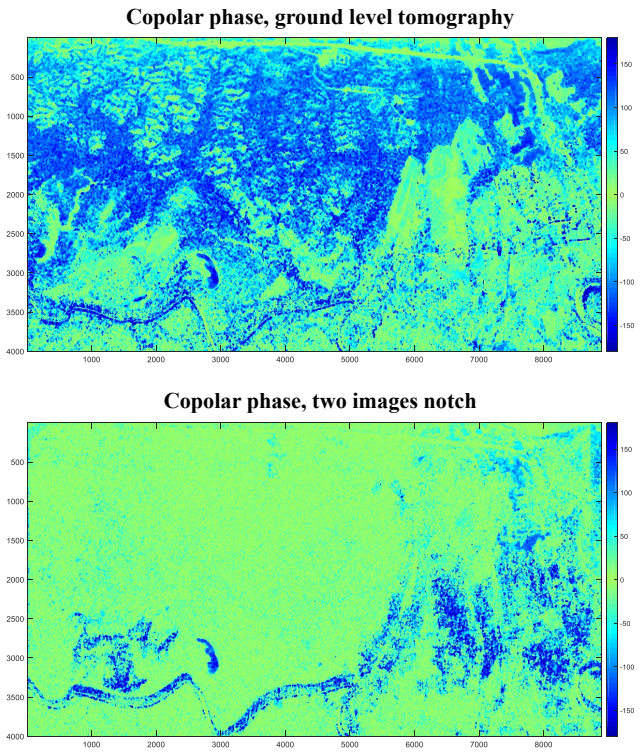

Fig. 2. Phase difference between HH and VV polarimetric channels. Above: ground level as seen through six images SAR tomography. Below: two images ground notch. ONERA TropiSAR, Paracou.

double bounce scattering mechanism [10]. The ground and tree act as a dihedral, thus providing strong echo and phase opposition between HH and VV polarimetric channels. The copolar phase (defined as the phase difference between HH and VV channels) is indeed a reliable indicator of the presence of double bounce. Copolar phase close to zero is typical of single bounces (such as rough surface backscattering) or volumetric scattering. In figure (2) two copolar phase maps are shown: the top one is associated with the ground level image as seen through tomography whereas the bottom one is associated with the notch image.

Analysis of the copolar phase suggests that P-band signals can effectively penetrate dense forests and reach the ground. Also, even in a medium as complex as a tropical forest, the effect associated with the 90° angle formed by soil and trunks can be clearly observed. The phase center of the dihedral is at ground level so its contribution can be effectively removed by zeroing the echo coming from the ground. The bottom panel of figure (2) shows that after notch processing the copolar phase is nearly zero in every part of the image. The upper left quarter of the image in particular is characterized by very dense forest: the double bounce almost completely vanishes.

Double bounce provides a strong echo only when the ground is flat; as the ground slope increases, the double bounce fades

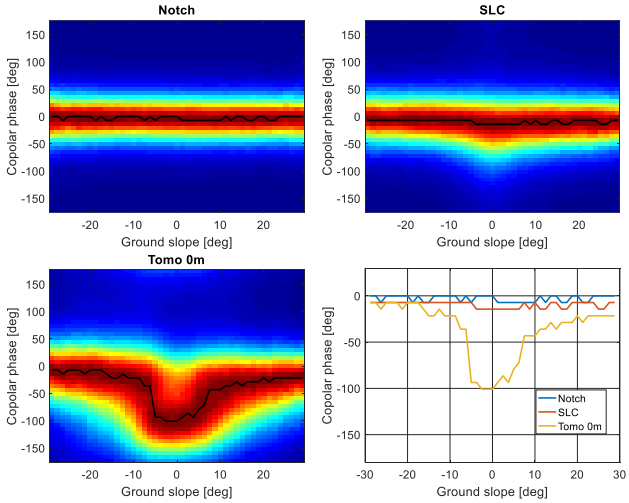

Fig. 3. Histograms relating copolar phase and ground slope. Each column of the histograms has been normalized with respect to maximum.

away. This can be observed by correlating the copolar phase with the ground slope. The bottom panel of figure (3) shows the sharp deviation from zero degrees when the surface slope approaches zero. Such clear behavior can be observed only in a tomographic image. The corresponding diagram for a fully polarimetric SLC image shown in the central panel of figure (3) exhibits only a slight shift of the peak around zero. The top panel shows the result of notch processing: flat areas cannot be distinguished from tilted ones and the copolar phase is stable on zero.

PolSAR images have been widely used to estimate AGB. Most models represent received power as an incoherent sum of surface scattering, double bounce and volumetric scattering, but the interaction of the electromagnetic wave with the forest is ruled by several parameters unconnected with AGB. Surface scattering is sensitive to AGB due to attenuation by the forest layer but it also depends on surface roughness and moisture. The double bounce power can be modeled as a complex function of AGB: on the one hand it increases with AGB as one bounce out of two involves the tree itself, but on the other hand it decreases with AGB due to the attenuation given by the forest layer. Notch processing provides the rejection of these scattering mechanisms thus returning volume-only components. This results in higher correlation and sensitivity to AGB as shown in figure (4).

4. CONCLUSIONS

This paper presents a new interferometric processing algorithm: InSAR ground notching. It exploits two coherent SAR images to cancel out the echo coming from targets at a given elevation above ground level. Its main use is to analyze im-

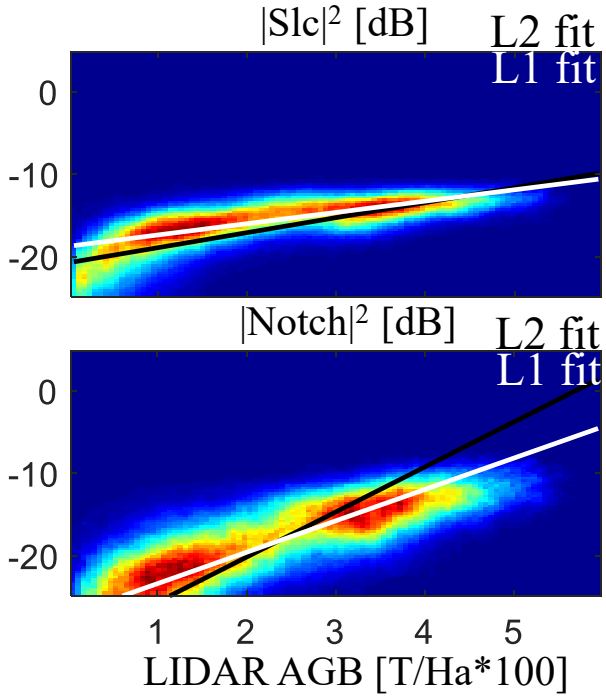

Fig. 4. Notch processing returns higher correlation with biomass than single look complex images. HV polarimetric channel shown here. DLR AfriSAR, Mondah.

ages gathered on semi-transparent targets, characterized by significant extension in the vertical direction. Notch processing allows an echo coming from a specific depth to be canceled out, making interpretation of the residual power easier. It has been successfully tested on forested areas to remove the contribution of the ground and ground-tree double bounce. Ground-free power exhibits greater correlation to AGB, thus making InSAR notching a very promising processing step in the algorithm for AGB estimation in the forthcoming ESA BIOMASS mission. A study that explicitly addresses AGB retrieval based on ground notched data is given in [11].

5. REFERENCES

[1] L. Villard and T. Le Toan, "Relating p-band sar intensity to biomass for tropical dense forests in hilly terrain: γ^0 or t^0?," *IEEE Journal of Selected Topics in Applied Earth Observations and Remote Sensing*, vol. 8, no. 1, pp. 214–223, Jan 2015.

[2] M. J. Soja, G. Sandberg, and L. M. H. Ulander, "Regression-based retrieval of boreal forest biomass in sloping terrain using p-band sar backscatter intensity data," *IEEE Transactions on Geoscience and Remote Sensing*, vol. 51, no. 5, pp. 2646–2665, May 2013.

[3] E. Blomberg, L. Ferro-Famil, M. J. Soja, L. M. H. Ulander, , and S. Tebaldini, "Forest biomass retrieval from l-band sar using tomographic ground backscatter removal," *IEEE Geoscience and Remote Sensing Letters*, p. Submitted, 2018.

[4] D. Ho Tong Minh, T. L. Toan, F. Rocca, S. Tebaldini, M. M. d'Alessandro, and L. Villard, "Relating p-band synthetic aperture radar tomography to tropical forest biomass," *IEEE Transactions on Geoscience and Remote Sensing*, vol. 52, no. 2, pp. 967–979, Feb 2014.

[5] S. Tebaldini, F. Rocca, M. Mariotti d'Alessandro, and L. Ferro-Famil, "Phase calibration of airborne tomographic sar data via phase center double localization," *IEEE Transactions on Geoscience and Remote Sensing*, vol. 54, no. 3, pp. 1775–1792, March 2016.

[6] S. Tebaldini, "Algebraic synthesis of forest scenarios from multibaseline polinsar data," *IEEE Transactions on Geoscience and Remote Sensing*, vol. 47, no. 12, pp. 4132–4142, Dec 2009.

[7] P. C. Dubois-Fernandez, T. Le Toan, S. Daniel, H. Oriot, J. Chave, L. Blanc, L. Villard, M. W. J. Davidson, and M. Petit, "The tropisar airborne campaign in french guiana: Objectives, description, and observed temporal behavior of the backscatter signal," *IEEE Transactions on Geoscience and Remote Sensing*, vol. 50, no. 8, pp. 3228–3241, Aug 2012.

[8] I. Hajnsek, M. Pardini, R. Horn, R. Scheiber, K. Papathanassiou, P. Dubois Fernandez, R. Baque, X. Dupuis, and T. Casal, "Sar imaging of tropical african forests with p-band multibaseline acquisitions: Results from the afrisar campaign," in *2016 IEEE International Geoscience and Remote Sensing Symposium (IGARSS)*, July 2016, pp. 7521–7523.

[9] N. Labrière et al., "In situ data from the tropisar and afrisar campaigns as a support to upcoming spaceborne biomass missions," *IEEE Transactions on Geoscience and Remote Sensing*, Submitted.

[10] M. M. d'Alessandro, S. Tebaldini, and F. Rocca, "Phenomenology of ground scattering in a tropical forest through polarimetric synthetic aperture radar tomography," *IEEE Transactions on Geoscience and Remote Sensing*, vol. 51, no. 8, pp. 4430–4437, Aug 2013.

[11] M. Soja, M. Mariotti d'Alessandro, S. Quegan, S. Tebaldini, and L. M. H. Ulander, "Model-based estimation of tropical forest biomass from notch-filtered p-band sar backscatter," in *2018 IEEE International Geoscience and Remote Sensing Symposium (IGARSS)*, July 2018, p. Submitted.